

A high order approach for anomalous sub-diffusion equation

Zongze Yang^a, Jungang Wang^{a,*}, Zhanbin Yuan^a, Yufeng Nie^a

^a*Department of Applied Mathematics, Northwestern Polytechnical University, Xi'an, Shanxi 710072, China*

Abstract

In this paper we are concerned with anomalous sub-diffusion equation, which describes the anomalous diffusion phenomenon in nature. Based on an equivalent transformation of equation and a smoothing transformation, we propose high order schemes combining Nyström method in temporal direction with compact finite difference method and spectral method in spatial direction. The idea of smoothing transformation is inspired by the method for Volterra integral equation proposed by P. Baratella and A. P. Orsi (2004). The advantage of this approach is that it can get good convergence rate even though the solution is less regularity on starting point, while most of current methods cannot handle this situation properly. The effectiveness of our methods are shown by numerical experiments.

Keywords: fractional derivative, anomalous sub-diffusion, weakly singular, Volterra integral equation

1. Introduction

Fractional calculus is an area having a long history, which is believed to have stemmed from a question about the meaning of notation $d^{\frac{1}{2}}y/dx^{\frac{1}{2}}$ raised in the year 1695 by Marquis de L'Hôpital to Gottfried Wilhelm Leibniz. During the past three decades or so, this subject has gained considerable popularity due mainly to its powerful applications in numerous seemingly diverse and widespread fields of science and engineering, such as materials and mechanics, signal processing, anomalous diffusion, biological systems, finance and so on (see [1, 2, 3, 4, 5, 6]). Now, there have been many papers presenting fractional calculus models for kinetics of natural anomalous processes in complex systems, and these models maintain the long-memory and non-local properties of the corresponding dynamics. Because of these properties, it is not easy to find the exact

*Corresponding author

Email addresses: zzyang@mail.nwpu.edu.cn (Zongze Yang), wangjungang@nwpu.edu.cn (Jungang Wang)

or numerical solutions of these equations, though researchers have developed many methods to approach this goal.

Special interest has been paid to the anomalous diffusion processes, which include super-slow diffusion (or sub-diffusion) and super-fast diffusion (or super-diffusion). Among those models, Anomalous sub-diffusion equations are some important. In this paper, we consider the following anomalous sub-diffusion problem[7]:

$$\begin{cases} u_t(x, t) = {}^{RL}_0\mathcal{D}_t^{1-\gamma}(Lu(x, t) + f(x, t)), & 0 < x \leq X, 0 < t \leq T \\ u(x, 0) = \varphi(x), & 0 \leq x \leq X, \\ u(0, t) = \psi_1(t), u(X, t) = \psi_2(t), & 0 \leq t \leq T, \end{cases} \quad (1.1)$$

where $0 < \gamma < 1$, $Lu(x, t) = K_\gamma u_{xx}(x, t)$ and ${}^{RL}_0\mathcal{D}_t^{1-\gamma}$ denotes the Riemann-Liouville fractional derivative of order $1 - \gamma$ defined by

$${}^{RL}_0\mathcal{D}_t^{1-\gamma}u(x, t) = \frac{1}{\Gamma(\gamma)} \frac{\partial}{\partial t} \int_0^t (t - \eta)^{\gamma-1} u(x, \eta) d\eta. \quad (1.2)$$

In some references, equation (1.1) is called the time Riemann-Liouville type sub-diffusion equation. Some researchers use an equivalent model instead of equation (1.1), that is

$${}^{RL}_0\mathcal{D}_t^\gamma u(x, t) = Lu(x, t) + f(x, t). \quad (1.3)$$

In fact, these two models are equivalent under some assumptions, for example, $u(x, 0) = 0$, which is a sufficient condition.

Many numerical methods have been developed to solve anomalous sub-diffusion equations. In 2005, Yuste and Scedo [8] proposed an explicit FTCS scheme, which combined the forward time centered space (FTCS) method with the Grünwald-Letnikov discretization of the Riemann-Liouville derivative. In the paper, they analysed the stability by a new von Neumann-type method. Zhuang et al. [7] presented an implicit numerical method and two techniques for improving the order of convergence. He also gave a stability and convergence analysis for the implicit numerical method but by energy method. Gao and Sun [9] established a compact finite difference scheme by using the L1 discretization for time-fractional part and fourth-order accuracy compact approximation for space derivative. In [10], Zeng et al. used linear multistep method and finite element method to approach time-fractional sub-diffusion equation, and got two unconditionally stable schemes. Gao et al. [11] obtained a scheme with global second-order numerical accuracy in time independent of the fractional derivative exponent. Recently, Zheng et al. [12] developed a high order scheme for multi-term time-fractional diffusion equation possessing high efficiency and exponential decay in both time and space directions.

There have been a great deal of researches on anomalous sub-diffusion equations, however, as noticed in [11], when the solution is not smooth enough at $t = 0$, the convergence rate will be lower than their expectations, even cannot

be solved by some methods. To overcome this shortcoming, we adopt some techniques similar to those used to deal with weakly singularity Volterra integral equation [13, 14]. By these techniques, we obtain better results even for the solution with weak regularity.

The outline of this paper is arranged as follows. In Section 2, we give an equivalent form of equation (1.1) by equivalent transformation and smoothing method, which can improve the regularity of the solution. In section 3, a semi-discrete scheme is given by discretizing the equivalent equation with Nyström method. And two fully-discrete schemes are given in section 4. Some numerical examples are present in Section 5 to show the efficiencies of those proposed schemes. Conclusion and some remarks are given in the last section.

2. Equivalent transformation and smoothing method

In paper [13], the authors proposed a simple smooth transformation for Volterra integral equations, which can improve the regularity of the solution and can be used to construct high order methods. In this section, we mainly introduce the smoothing method used to transform the original fractional differential equation (1.1).

In order to use the smoothing method, the equation should be transformed into an integral equation. So we transform (1.1) into an integral equation by integrating both sides of it

$$u(x, t) = u(x, 0) + \frac{1}{\Gamma(\gamma)} \int_0^t (t - \eta)^{\gamma-1} (Lu(x, \eta) + f(x, \eta)) d\eta. \quad (2.1)$$

The last term in the right hand has a similar form with the integral term in Volterra integral equation. Following [13], introduce the smooth transformation

$$\lambda(t) = (b - a)^{1-q} (t - a)^q + a, \quad q \in \{1, 2, \dots, n, \dots\}, \quad (2.2)$$

which maps $[a, b]$ into $[a, b]$, where $a = 0$, $b = T$. We use a , b as end points in order to state the generality of the transformation. Let $\alpha = 1 - \gamma$ and change variables in (2.1) by setting $\eta = \lambda(s)$, $t = \lambda(t')$. Replacing t' by t , then we have

$$u(x, \lambda(t)) = u(x, \lambda(a)) + \frac{1}{\Gamma(\gamma)} \int_a^t (\lambda(t) - \lambda(s))^{-\alpha} G(x, s) \lambda'(s) ds, \quad (2.3)$$

where $G(x, s) = Lu(x, \lambda(s)) + f(x, \lambda(s))$. To transform the kernel of (2.3) with form $(t - s)^{-\alpha}$, define [13]

$$\delta_\alpha(t, s) = \begin{cases} \left(\frac{(t - a)^q - (s - a)^q}{t - s} \right)^{-\alpha}, & t \neq s, \\ (q(s - a)^{q-1})^{-\alpha}, & t = s. \end{cases} \quad (2.4)$$

And (2.4) implies

$$(\lambda(t) - \lambda(s))^{-\alpha} = ((b - a)^{1-q})^{-\alpha} \delta_\alpha(t, s) (t - s)^{-\alpha}. \quad (2.5)$$

Now, multiplying both sides of (2.3) by $\lambda'(t)$, we can rewrite (2.3) as

$$\lambda'(t)u(x, \lambda(t)) = \lambda'(t)u(x, \lambda(a)) + \frac{1}{\Gamma(\gamma)} \int_a^t (t-s)^{-\alpha} K_\alpha(t, s) G(x, s) \lambda'(s) ds \quad (2.6)$$

where

$$K_\alpha(t, s) = ((b-a)^{1-q})^{-\alpha} \lambda'(t) \delta_\alpha(t, s). \quad (2.7)$$

In order to use Nyström method in spatial direction, we introduce another transformation $\mu(t) = \frac{b-a}{2}t + \frac{b+a}{2}$ and denote

$$\begin{cases} v(x, t) = \lambda'(\mu(t))u(x, \lambda(\mu(t))), \\ g(x, t) = \lambda'(\mu(t))f(x, \lambda(\mu(t))), \\ h(x, t) = \lambda'(\mu(t))u(x, \lambda(a)). \end{cases} \quad (2.8)$$

By setting $t = \mu(t')$, $s = \mu(s')$ in (2.6), and replacing t' by t , s' by s , we get

$$v(x, t) = h(x, t) + \frac{1}{\Gamma(\gamma)} \int_{-1}^t (t-s)^{-\alpha} H(t, s) (Lv(x, s) + g(x, s)) ds, \quad (2.9)$$

where

$$H(t, s) = \left(\frac{b-a}{2}\right)^{1-\alpha} K_\alpha(\mu(t), \mu(s)). \quad (2.10)$$

After two times transformation, a new equation (2.9) of problem (1.1) is derived. Though equation (2.9) still has weakly singular kernel, the smoothness of the solution increase with q . So some method, which cannot working before, can be applied for solving it.

As a conclusion, we illustrate the smoothing process as below

$$\begin{array}{ccc} u(x, t) & \xrightarrow{\lambda(s)=(b-a)^{1-q}(s-a)^q+a} & u(x, \lambda(s)) \\ & & \downarrow \times \lambda'(s) \\ v(x, r) & \xleftarrow[\mu(r)=\frac{b-a}{2}r+\frac{b+a}{2}]{s=\mu(r)} & \lambda'(s)u(x, \lambda(s)) \end{array}$$

In the next section, we will introduce how to discrete it.

3. The semi-discrete approximation

In previous section we have obtained a smoothed equation (2.9). Here, we present a semi-discrete scheme by Nyström method.

Choose $N+1$ distinct points $\tau_n, n=0, \dots, N$ in the interval $[-1, 1]$ corresponding to $t_n, n=0, \dots, N$ in $[a, b]$ with $t_n = \lambda(\mu(\tau_n))$. And collocate the equation at the nodes $\{\tau_n\}_{n=0}^N$

$$v(x, \tau_n) = h(x, \tau_n) + \frac{1}{\Gamma(\gamma)} \int_{-1}^{\tau_n} (\tau_n - s)^{-\alpha} H(\tau_n, s) (Lv(x, s) + g(x, s)) ds. \quad (3.1)$$

Then replace $H(\tau_n, s)(Lv(x, s) + g(x, s))$ by the corresponding Lagrange interpolation polynomials associated with $\{\tau_n\}_{n=0}^N$

$$v(x, \tau_n) = h(x, \tau_n) + \frac{1}{\Gamma(\gamma)} \sum_{j=0}^N w_{n,j} H(\tau_n, \tau_j) (Lv(x, \tau_j) + g(x, \tau_j)) \quad (3.2)$$

where

$$w_{n,j} = \int_{-1}^{\tau_n} (\tau_n - s)^{-\alpha} I_{N,j}(s) ds,$$

and $I_{N,j}(s)$ are the Lagrange interpolation polynomials on points $\{\tau_n\}_{n=0}^N$. For the computation of the coefficients of $w_{n,j}$, we use Jacobi-Gauss quadrature as described in [15].

Remark 3.1. *The point $\tau = -1$ should not be chosen as a node of $\{\tau_n\}$ because of the singularity of the solution.*

Remark 3.2. *By choosing different $\{\tau_n\}_{n=0}^N$, we get different approximation polynomials with different accuracy. This will have effect on the accuracy of the solution.*

Then, we obtain a semi-discrete scheme for equation (1.1)

$$v(x, \tau_n) = h(x, \tau_n) + \sum_{j=0}^N r_{nj} (Lv(x, \tau_j) + g(x, \tau_j)), \quad (3.3)$$

$$n = 0, 1, \dots, N,$$

where $r_{nj} = w_{n,j} H(\tau_n, \tau_j) / \Gamma(\gamma)$. Once $v(x, \tau)$ is obtained, the solution of the original equation is given by

$$u(x, t) = \frac{v(x, \tau)}{\lambda'(\mu(\tau))}, \quad t = \lambda(\mu(\tau)). \quad (3.4)$$

4. The fully-discrete approximation

Because of the high convergence rate in temporal direction of the scheme, we need high order method in spatial direction to fit it. In this section, we perform two different discrete methods on spatial variable.

4.1. Discrete spatial variable by compact difference operator

In this subsection, we use spatial compact approximation in spatial direction.

Let $x_k = k\Delta x$, ($k = 0, 1, \dots, M$) with step $\Delta x = X/M$. Like [11], denote a average operator

$$\mathcal{A}u_i = \begin{cases} (I + \frac{\Delta x^2}{12} \delta_x^2)u_i, & 1 \leq i \leq M-1, \\ u_i, & i = 0 \text{ or } i = M. \end{cases} \quad (4.1)$$

where δ_x^2 is center difference operator.

Perform \mathcal{A} on both side of (3.3) at $\{x_k\}_{k=1}^{M-1}$

$$\mathcal{A}v(x_k, \tau_n) = \mathcal{A}h(x_k, \tau_n) + \sum_{j=0}^N r_{nj} (K_\gamma \mathcal{A}v_{xx}(x_k, s) + \mathcal{A}g(x_k, s)) ds. \quad (4.2)$$

The next thing is to approximation $\mathcal{A}v_{xx}(x_k, s)$. In order to obtain the spatial compact scheme, we need the following lemma, which suggests that $\delta_x^2 v(x_k, s)$ is good approximation to $\mathcal{A}v_{xx}(x_k, s)$.

Lemma 4.1 ([11]). *Let function $g(x) \in C^6[0, X]$ and*

$$\xi(\eta) = (1 - \eta)^3 (5 - 3(1 - \eta)^2).$$

Then

$$\mathcal{A}g''(x_i) = \delta_x^2 g(x_i) + \frac{\Delta x^4}{360} \int_0^1 (g^{(6)}(x_i - \eta \Delta x) + g^{(6)}(x_i + \eta \Delta x)) \xi(\eta) d\eta. \quad (4.3)$$

By Lemma 4.1, we have

$$\mathcal{A}v(x_k, \tau_n) = \mathcal{A}h(x_k, \tau_n) + r_{nj} (K_\gamma \delta_x^2 v(x_k, \tau_j) + \mathcal{A}g(x_k, \tau_j)) + O(\Delta x^4). \quad (4.4)$$

Drop down the high order term, hence

$$\mathcal{A}v(x_k, \tau_n) = \mathcal{A}h(x_k, \tau_n) + r_{nj} (K_\gamma \delta_x^2 v(x_k, \tau_j) + \mathcal{A}g(x_k, \tau_j)). \quad (4.5)$$

So we establish the fully-discrete scheme by discrete spatial variables with compact difference operator.

Now we introduce the matrix form of the last scheme. Denote $v_k^n = v(x_k, \tau_n)$, $h_k^n = h(x_k, \tau_n)$, and $g_k^j = g(x_k, \tau_j)$. We can write the matrix form as below:

$$\begin{aligned} \mathbf{V} + \frac{1}{12}(\mathbf{D}\mathbf{V} + \mathbf{B}) &= \mathbf{V}_0 + \frac{1}{12}(\mathbf{D}\mathbf{V}_0 + \mathbf{B}_0) \\ &+ \frac{K_\gamma}{\Delta x^2}(\mathbf{D}\mathbf{V} + \mathbf{B})\mathbf{W}^T + (\mathbf{G} + \frac{1}{12}(\mathbf{D}\mathbf{G} + \mathbf{B}_g))\mathbf{W}^T \end{aligned} \quad (4.6)$$

where

$$\begin{aligned} (\mathbf{V})_{k,n+1} &= v_k^n, & (\mathbf{V}_0)_{k,n+1} &= h_k^n, \\ (\mathbf{W})_{n+1,j+1} &= r_{nj}, & (\mathbf{G})_{k,n+1} &= g_k^n, \end{aligned} \quad (4.7)$$

with $k = 1, \dots, M-1$, $j = 0, \dots, N$, $n = 0, \dots, N$ and

$$\mathbf{D}_{(M-1) \times (M-1)} = \text{tridiag}(1, -2, 1),$$

$$\mathbf{B}_{(M-1) \times (N+1)} = \begin{pmatrix} v_0^0 & v_0^1 & \cdots & v_0^{N-1} & v_0^N \\ 0 & 0 & \cdots & 0 & 0 \\ \vdots & \vdots & \ddots & \vdots & \vdots \\ 0 & 0 & \cdots & 0 & 0 \\ v_M^0 & v_M^1 & \cdots & v_M^{N-1} & v_M^N \end{pmatrix},$$

$$\begin{aligned}
\mathbf{B}_{0,(M-1) \times (N+1)} &= \begin{pmatrix} h_0^0 & h_0^1 & \cdots & h_0^{N-1} & h_0^N \\ 0 & 0 & \cdots & 0 & 0 \\ \vdots & \vdots & \ddots & \vdots & \vdots \\ 0 & 0 & \cdots & 0 & 0 \\ h_M^0 & h_M^1 & \cdots & h_M^{N-1} & h_M^N \end{pmatrix}, \\
\mathbf{B}_{g,(M-1) \times (N+1)} &= \begin{pmatrix} g_0^0 & g_0^1 & \cdots & g_0^{N-1} & g_0^N \\ 0 & 0 & \cdots & 0 & 0 \\ \vdots & \vdots & \ddots & \vdots & \vdots \\ 0 & 0 & \cdots & 0 & 0 \\ g_M^0 & g_M^1 & \cdots & g_M^{N-1} & g_M^N \end{pmatrix}.
\end{aligned}$$

To simplify, we recombine the terms in equation (4.6) as

$$\mathbf{T}\mathbf{V} - \mathbf{A}\mathbf{V}\mathbf{W}^T = \mathbf{S}, \quad (4.8)$$

where $\mathbf{T} = \mathbf{I} + \frac{1}{12}\mathbf{D}$, $\mathbf{A} = \frac{K_\gamma}{\Delta x^2}\mathbf{D}$ and

$$\mathbf{S} = -\frac{1}{12}\mathbf{B} + \mathbf{V}_0 + \frac{1}{12}(\mathbf{D}\mathbf{V}_0 + \mathbf{B}_0) + \left(\mathbf{G} + \frac{1}{12}(\mathbf{D}\mathbf{G} + \mathbf{B}_g)\right)\mathbf{W}^T. \quad (4.9)$$

Combining (3.4) and (4.8), we can obtain the solution of the original equation.

4.2. Spatial discretization with spectral method

In order to compare the result with some exist algorithms, we use the space basis function, presented by Zheng et al. in [12], to solve equation (3.3). Here we just process zero boundary condition, i.e., $u(0, t) = 0$, $u(X, t) = 0$.

First, let us state the variational problem of equations (3.3). We recall semi-discrete scheme (3.3) here:

$$\begin{aligned}
v(x, \tau_n) &= h(x, \tau_n) + \sum_{j=0}^N r_{nj}(Lv(x, \tau_j) + g(x, \tau_j)) \\
n &= 0, 1, \dots, N,
\end{aligned} \quad (4.10)$$

Set $v^n(x) = v(x, \tau_n)$, $h^n(x) = h(x, \tau_n)$, $g^n(x) = g(x, \tau_n)$, $\Lambda = [0, X]$. Then the variational problem of (3.3) is : Find $v^n(x) \in H_0^1(\Lambda)$, ($n = 0, 1, \dots, N$) for $\forall \phi(x) \in H_0^1(\Lambda)$, such that

$$\begin{aligned}
& (v^n(x), \phi(x)) + K_\gamma \sum_{j=0}^N r_{nj}(v_x^j(x), \phi_x(x)) \\
&= (h^n(x), \phi(x)) + \sum_{j=0}^N r_{nj}(g^j(x), \phi(x)).
\end{aligned} \quad (4.11)$$

Next, we construct spectral scheme for the above variational problem. Let $\mathbb{P}_{M'}(\Lambda)$ denotes the spaces of polynomials of degree up to M' . And set

$$P_{M'}(\Lambda) = \{p(x) \in \mathbb{P}_{M'}(\Lambda) | p(0) = p(X) = 0\}.$$

Adopt the Fourier-like functions proposed by Zheng et al. [12, see Section 4.2 for more details]:

$$\zeta_i(x) (i = 0, 1, \dots, M' - 2), x \in \Lambda$$

And the basis functions $\zeta_i(x)$ have the following property.

Lemma 4.2 ([12]). *For the basis functions $\zeta_i(x) (i = 0, 1, \dots, M' - 2), x \in (a, b)$,*

$$(\zeta_i(x), \zeta_j(x)) = \pi_i \delta_{ij}, \quad (\zeta'_i(x), \zeta'_j(x)) = \delta_{ij}. \quad (4.12)$$

Remark 4.1. *Here the π_i is used to replace the τ_i in section 4.2 of paper [12].*

Let $v_L^n = \sum_{i=0}^{M'-2} \hat{v}_i^n \zeta_i$, then we obtain the spectral scheme for problem (4.11):

$$\begin{aligned} (v_L^n(x), \zeta_i(x)) + K_\gamma \sum_{j=0}^N r_{nj} (v_{L,x}^j(x), \zeta'_i(x)) \\ = (h^n(x), \zeta_i(x)) + \sum_{j=0}^N r_{nj} (g^j(x), \zeta_i(x)), \end{aligned} \quad (4.13)$$

$$\forall i = 0, 1, \dots, M' - 2.$$

Now, we introduce the matrix form of this scheme. Adopt the following notations

$$\begin{aligned} V^j &= (\hat{v}_0^j, \hat{v}_1^j, \dots, \hat{v}_{M'-2}^j)^T, \\ H^j &= ((h^j, \zeta^0), (h^j, \zeta^1), \dots, (h^j, \zeta^{M'-2}))^T, \\ G^j &= ((g^j, \zeta^0), (g^j, \zeta^1), \dots, (g^j, \zeta^{M'-2}))^T, \end{aligned} \quad (4.14)$$

Then we have

$$\mathbf{\Pi} V^n + K_\gamma \sum_{j=0}^N r_{nj} V^j = H^n + \sum_{j=0}^N r_{nj} G^j, \quad n = 0, 1, \dots, N, \quad (4.15)$$

where $\mathbf{\Pi} = \text{diag}(\pi_0, \pi_1, \dots, \pi_{M'-2})$. Also define

$$\begin{aligned} V &= (V^{0T}, V^{1T}, \dots, V^{NT})^T, \\ H &= (H^{0T}, H^{1T}, \dots, H^{NT})^T, \\ G &= (G^{0T}, G^{1T}, \dots, G^{NT})^T, \end{aligned} \quad (4.16)$$

Then the matrix form of this scheme is

$$(\mathbf{A} + K_\gamma \mathbf{B})V = H + \mathbf{B}G \quad (4.17)$$

where $\mathbf{A} = \mathbf{I}_{N+1} \otimes \mathbf{\Pi}$, $\mathbf{B} = \mathbf{W} \otimes \mathbf{I}_{M'-1}$, and \mathbf{I}_{N+1} , along with $\mathbf{I}_{M'-1}$, are identity matrices.

Table 1: Errors and spatial convergence order with $c = 1.9$, $\gamma = 0.6$, $N = 100$

M	$q = 1$		$q = 2$		$q = 3$	
	error	order	error	order	error	order
10	2.11e-08		2.11e-08		2.11e-08	
20	1.32e-09	4.00	1.32e-09	4.00	1.32e-09	4.00
30	2.60e-10	4.00	2.60e-10	4.00	2.60e-10	4.00
40	8.23e-11	4.00	8.23e-11	4.00	8.23e-11	4.00
50	3.37e-11	4.00	3.37e-11	4.00	3.37e-11	4.00

Table 2: Errors and spatial convergence order with $c = 0.1$, $\gamma = 0.6$, $N = 100$

M	$q = 1$		$q = 2$		$q = 3$	
	error	order	error	order	error	order
10	2.58e-08		2.27e-08		2.27e-08	
20	4.76e-09	2.44	1.42e-09	4.00	1.42e-09	4.00
30	4.21e-09	0.30	2.80e-10	4.00	2.81e-10	4.00
40	4.30e-09	-0.07	8.86e-11	4.00	8.88e-11	4.00
50	4.23e-09	0.07	3.62e-11	4.02	3.64e-11	4.00

5. Numerical results

In this section, we present some examples to illustrate the accuracy of our methods.

Example 5.1. Consider equation (1.1) with $X = 1$, $T = 1$, and

$$\begin{cases} u(x, 0) = 0, \\ u(0, t) = 0, \quad u(1, t) = t^{c+\gamma} \sin 1, \\ f(x, t) = (k_\gamma t^c + t^{c+\gamma}) \sin x, \end{cases} \quad (5.1)$$

where $k_\gamma = \frac{\Gamma(c+\gamma+1)}{\Gamma(c+1)}$ and $K_\gamma = 1$. The exact solution under these conditions is

$$u(x, t) = t^{c+\gamma} \sin x.$$

In this example, we investigate the convergence order of scheme (4.5). The high convergence order can be easily seen from Table 1, in which we take $c = 1.9$, $\gamma = 0.6$, and $N = 100$. Table 2 shows the effect of smoothing method with different q for equation (1.1) with $c = 0.1$, $\gamma = 0.6$, and $N = 100$. It also shows that the convergence order in space is significantly improved when $q = 2$. As shown in Table 3 and 4, convergence rate in time can be improved in various degree when exact solutions have different regularity. These results indicates that the smoothing method can retain the convergence order when the regularity of u is low.

Table 3: Maximum errors with $c = 1.4$, $\gamma = 0.8$, $M = 5000$

N	6	8	10	12	14
$q = 1$	3.20e-06	6.91e-07	2.09e-07	7.76e-08	3.33e-08
$q = 2$	2.37e-07	1.08e-08	9.91e-10	1.42e-10	3.12e-11
$q = 3$	5.44e-07	3.26e-09	7.84e-11	2.13e-12	1.45e-12

Table 4: Maximum errors with $c = 0.5$, $\gamma = 0.8$, $M = 5000$

N	6	8	10	12	14
$q = 1$	2.87e-05	1.00e-05	4.39e-06	2.22e-06	1.24e-06
$q = 2$	1.68e-07	1.84e-08	3.45e-09	8.72e-10	2.70e-10
$q = 3$	3.96e-07	2.22e-08	2.19e-09	3.42e-10	6.34e-11

Table 5: Maximum errors with $c = 3.1$, $\gamma = 0.5$, $M = 5000$

N	6	8	10	12	14
$q = 1$	7.23e-08	6.42e-09	1.03e-09	2.82e-10	1.03e-10
$q = 2$	4.90e-06	5.38e-09	4.49e-11	4.82e-12	2.46e-12
$q = 3$	2.85e-04	4.79e-06	3.32e-09	1.64e-11	3.13e-12

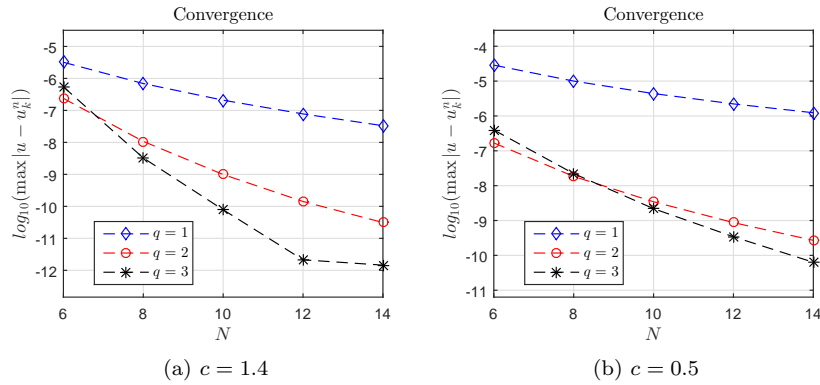


Figure 1: Convergence of scheme (4.5) for different c with $\gamma = 0.8$, $M = 10000$.

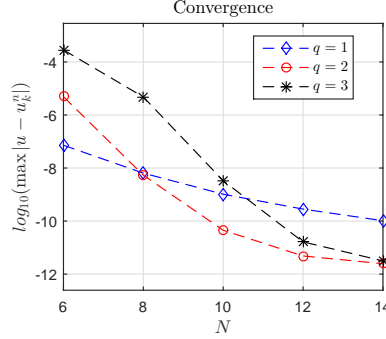


Figure 2: Convergence of scheme (4.5) with $c = 3.1$, $\gamma = 0.5$, $M = 10000$.

Maximum errors for different N are shown in Figure 1 with $c = 1.4$, $\gamma = 0.8$ and $c = 0.5$, $\gamma = 0.8$ separately. The Figure 2 shows that the convergence rate increase as q increase. The results shown in these figures, along with the results in Table 5, suggests that it is profitable to perform smooth transformation on the equation no matter what regularity the solution has.

Example 5.2. In this example, we Consider equation (1.1) with $X = 1$, $T = 1$, and

$$\begin{cases} u(x, 0) = 0, \\ u(0, t) = 0, \quad u(1, t) = 0, \\ f(x, t) = (k_\gamma t^c + \pi^2 t^{c+\gamma}) \sin \pi x, \end{cases} \quad (5.2)$$

where $k_\gamma = \frac{\Gamma(c+\gamma+1)}{\Gamma(c+1)}$ and $K_\gamma = 1$. The exact solution of equation (1.1) is

$$u(x, t) = t^{c+\gamma} \sin \pi x.$$

It is also the solution of equation in the following form:

$$\begin{cases} {}^{RL}_0\mathcal{D}_T^\gamma u = u_{xx} + f \\ u(x, 0) = 0, u(t, 0) = 0, u(t, 1) = 0, \\ f = k_\gamma t^c \sin \pi x + \pi^2 t^{c+\gamma} \sin \pi x, \end{cases} \quad (5.3)$$

This equation is equivalent with our equation (1.1). In [12], the authors solved sub-diffusion equations with this form. Here, we compare the numerical results of scheme (4.13) with the results of the method developed by Zheng et al. in [12], which possesses high efficiency and exponential decay in both time and space directions.

In this example we take $\gamma = 0.4$ and take the polynomials degree of spatial base $M' = 200$ to compute some results with different c . First, we choose $c = 2.5, 1.5$, and present the maximum errors in Table 6 and Table 7 respectively. In addition to visualize these data, we plot them in Figure 3. From those tables and figures, we can see that Zheng's result is close to our result with $q = 1$, and

Table 6: Maximum errors with $c = 2.5$, $\gamma = 0.4$, $M' = 200$

N	6	8	10	12	14
$q = 1$	4.87e-07	6.38e-08	1.26e-08	3.23e-09	1.00e-09
$q = 2$	5.31e-07	7.01e-09	1.80e-10	7.27e-12	4.90e-13
$q = 3$	7.60e-05	8.67e-08	7.51e-10	1.56e-11	3.13e-13
Zheng et al.	6.66e-06	9.98e-07	2.26e-07	6.62e-08	2.32e-08

 Table 7: Maximum errors with $c = 1.5$, $\gamma = 0.4$, $M' = 200$

N	6	8	10	12	14
$q = 1$	2.25e-06	5.10e-07	1.54e-07	5.58e-08	2.32e-08
$q = 2$	2.39e-07	7.95e-09	4.85e-10	5.31e-11	8.67e-12
$q = 3$	8.45e-07	1.28e-08	3.80e-10	2.61e-11	1.17e-12
Zheng et al.	3.60e-05	9.63e-06	3.38e-06	1.41e-06	6.67e-07

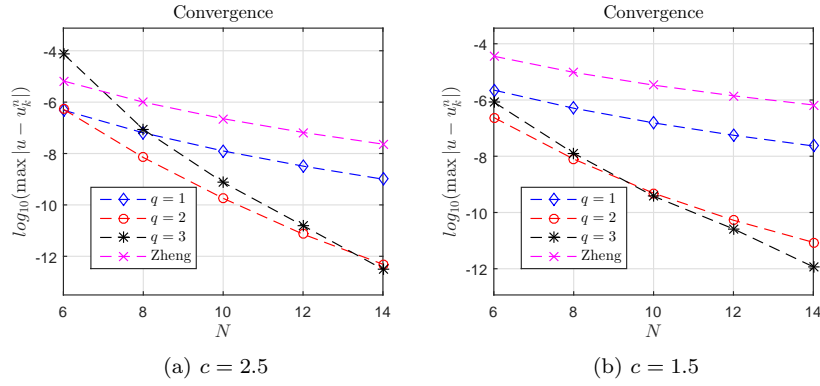

 Figure 3: Convergence of scheme (4.13) for different c with $\gamma = 0.4$, $M' = 200$.

 Table 8: Maximum errors with $c = 0.5$, $\gamma = 0.4$, $M' = 200$

N	10	18	26	34	42	50
$q = 1$	4.38e-06	4.64e-07	1.04e-07	3.39e-08	1.40e-08	6.76e-09
$q = 2$	1.27e-08	1.42e-10	7.00e-12	7.23e-13	1.19e-13	2.18e-14
$q = 3$	4.31e-09	1.51e-11	3.63e-13	2.32e-14	1.11e-15	1.22e-15
Zheng et al.	1.48e-04	2.56e-05	8.09e-06	3.42e-06	1.72e-06	9.68e-07

 Table 9: Maximum errors with $c = -0.1$, $\gamma = 0.4$, $M' = 200$

N	10	18	26	34	42	50
$q = 1$	1.95e-05	4.14e-06	1.50e-06	7.15e-07	4.05e-07	2.57e-07
$q = 2$	1.47e-06	9.93e-08	1.68e-08	4.50e-09	1.58e-09	6.71e-10
$q = 3$	1.57e-07	3.65e-09	3.22e-10	5.32e-11	1.27e-11	3.83e-12

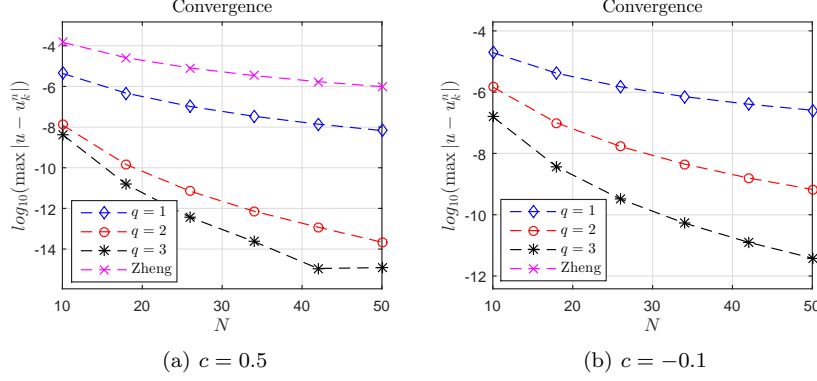


Figure 4: Convergence of scheme (4.13) for different c with $\gamma = 0.4$, $M' = 200$.

bigger q can significantly improve the accuracy. Also, notice that larger q can speed up the convergence.

Next, we choose $c = 0.5, -0.1$, and show the results in Table 8, Table 9, and Figure 4. Zheng's method cannot handle the situation with $c = -0.1$, so we just present our result in table and figure when $c = -0.1$. As c decrease, the regularity of the solution become weaker, and this result in slow convergence speed as shown in Figure 3 and Figure 4. However, we can still get accurate results by setting q larger. So it is recommended to apply smooth transformation on the equations.

Example 5.3. Consider anomalous sub-diffusion equation

$$\frac{\partial u}{\partial t} = \frac{\partial^{1-\gamma}}{\partial t^{1-\gamma}} \left(\frac{\partial^2 u}{\partial x^2} \right), \quad (5.4)$$

with initial and boundary conditions [7]

$$u(x, 0) = \begin{cases} 2x, & 0 \leq x \leq 0.5, \\ \frac{4-2x}{3}, & 0.5 \leq x \leq 2, \end{cases} \quad (5.5)$$

$$u(0, t) = u(2, t) = 0, \quad 0 \leq t \leq 0.4.$$

We simulate this system by scheme (4.5) with $N = 20, M = 20$. Figure 5 shows the numerical approximation $u(x, t)$ when $\gamma = 0.1$ and $\gamma = 0.9$ respectively. And Figure 6 illustrates the change of approximation $u(x, t)$ as γ vary in quantity. These results shows that the system exhibits sub-diffusion behaviors and the solution continuously depends on the time fractional derivative.

6. Conclusion

In this paper, a high order method has been proposed to solve anomalous sub-diffusion equations especially when the exact solution less regularity. In

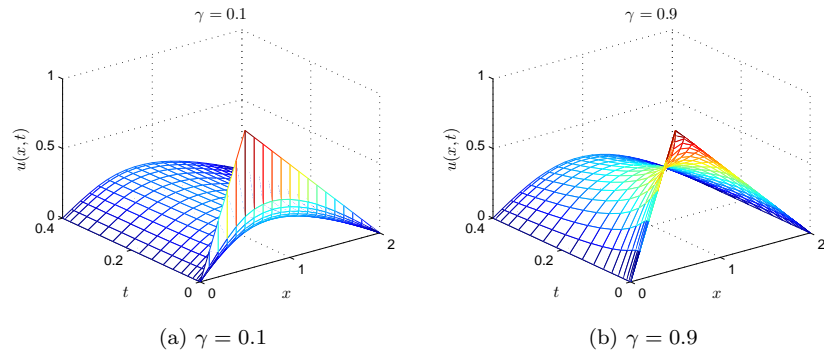


Figure 5: Numerical approximation of $u(x, t)$ for different γ when $N = 20, M = 20$.

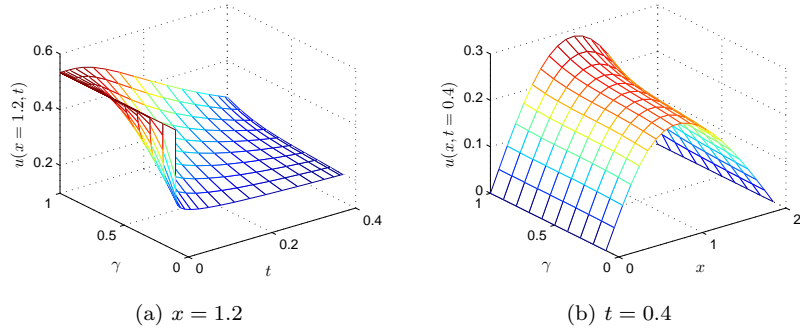


Figure 6: The numerical approximation $u(x, t)$ for various γ when $N = 20, M = 20$.

the numerical experiment, we have seen the effectiveness and accuracy of this method. And compact difference method used in spatial direction makes this method more effectively. However, theory analysis of convergence order and stability for this method is less, and the necessary or sufficient conditions are not clear. So, in the future, we will focus on the theory analysis of this method.

Acknowledgements

This research was supported by the National Natural Science Foundation of China (11471262), the Natural Science Foundation of Shaanxi Province (2014JM1028), the Fundamental Research Funds for the Central Universities (3102014JCQ01078) and the Center for high performance computing of Northwestern Polytechnical University.

Reference

References

- [1] G. M. Zaslavsky, Chaos, fractional kinetics, and anomalous transport, *Physics Reports* 371 (2002) 461–580. doi:10.1016/S0370-1573(02)00331-9.
- [2] S. Yuste, L. Acedo, Some exact results for the trapping of subdiffusive particles in one dimension, *Physica A: Statistical Mechanics and its Applications* 336 (3-4) (2004) 334–346. doi:10.1016/j.physa.2003.12.048.
- [3] R. Metzler, J. Klafter, The random walk’s guide to anomalous diffusion: a fractional dynamics approach, *Physics Reports* 339 (1) (2000) 1–77. doi:10.1016/S0370-1573(00)00070-3.
- [4] A. Cartea, D. del Castillo-Negrete, Fluid limit of the continuous-time random walk with general levy jump distribution functions, *Physical Review E* 76 (4, 1). doi:{10.1103/PhysRevE.76.041105}.
- [5] R. L. Magin, Fractional calculus models of complex dynamics in biological tissues, *Computers & Mathematics with Applications* 59 (5) (2010) 1586–1593, fractional Differentiation and Its Applications. doi:10.1016/j.camwa.2009.08.039.
- [6] R. Gorenflo, F. Mainardi, E. Scalas, M. Raberto, *Mathematical Finance: Workshop of the Mathematical Finance Research Project, Konstanz, Germany, October 5–7, 2000*, Birkhäuser Basel, Basel, 2001, Ch. Fractional Calculus and Continuous-Time Finance III : the Diffusion Limit, pp. 171–180. doi:10.1007/978-3-0348-8291-0_17.
- [7] P. Zhuang, F. Liu, V. Anh, I. Turner, New solution and analytical techniques of the implicit numerical method for the anomalous subdiffusion equation, *SIAM Journal on Numerical Analysis* 46 (2) (2008) 1079–1095. doi:10.1137/060673114.

- [8] S. B. Yuste, L. Acedo, An explicit finite difference method and a new von neumann-type stability analysis for fractional diffusion equations, *SIAM Journal on Numerical Analysis* 42 (5) (2005) 1862–1874. doi:10.1137/030602666.
- [9] G. Gao, Z. Sun, A compact finite difference scheme for the fractional sub-diffusion equations, *Journal of Computational Physics* 230 (3) (2011) 586–595.
- [10] F. Zeng, C. Li, F. Liu, I. Turner, The use of finite difference/element approaches for solving the time-fractional subdiffusion equation, *SIAM Journal on Scientific Computing* 35 (6) (2013) A2976–A3000.
- [11] G. Gao, H. Sun, Z. Sun, Stability and convergence of finite difference schemes for a class of time-fractional sub-diffusion equations based on certain superconvergence, *Journal of Computational Physics* 280 (2015) 510–528. doi:10.1016/j.jcp.2014.09.033.
- [12] M. Zheng, F. Liu, V. Anh, I. Turner, A high-order spectral method for the multi-term time-fractional diffusion equations, *Applied Mathematical Modelling* doi:10.1016/j.apm.2015.12.011.
- [13] P. Baratella, A. P. Orsi, A new approach to the numerical solution of weakly singular volterra integral equations, *Journal of Computational and Applied Mathematics* 163 (2) (2004) 401–418. doi:10.1016/j.cam.2003.08.047.
- [14] G. Monegato, I. H. Sloan, Numerical solution of the generalized airfoil equation for an airfoil with a flap, *SIAM Journal on Numerical Analysis* 34 (6) (1997) 2288–2305. doi:10.1137/S0036142995295054.
- [15] J. Shen, T. Tang, L.-L. Wang, *Spectral Methods: Algorithms, Analysis and Applications*, 1st Edition, no. 41 in Springer Series in Computational Mathematics, Springer-Verlag Berlin Heidelberg, 2011. doi:10.1007/978-3-540-71041-7.